AMERICAN SOCIETY FOR MICROBIOLOGY | mBio®

RESEARCH ARTICLE

Alveolar Type II Epithelial Cells Contribute to the Anti-Influenza A Virus Response in the Lung by Integrating Pathogen- and Microenvironment-Derived Signals

S. Stegemann-Koniszewski,[a,b] Andreas Jeron,[b] Marcus Gereke,[a,b] Robert Geffers,[c] Andrea Kröger,[d,e] Matthias Gunzer,[f] Dunja Bruder[a,b]

Immune Regulation, Helmholtz Centre for Infection Research, Braunschweig, Germany[a]; Infection Immunology, Institute of Medical Microbiology, Infection Control and Prevention, Otto-von-Guericke University, Magdeburg, Germany[b]; Genome Analytics, Helmholtz Centre for Infection Research, Braunschweig, Germany[c]; Innate Immunity and Infection, Helmholtz Centre for Infection Research, Braunschweig, Germany[d]; Molecular Microbiology, Institute of Medical Microbiology, Infection Control and Prevention, Otto-von-Guericke University, Magdeburg, Germany[e]; Institute of Experimental Immunology and Imaging, University of Duisburg-Essen, Essen, Germany[f]

S.S.-K. and A.J. contributed equally to this work.

ABSTRACT **Influenza A virus (IAV) periodically causes substantial morbidity and mortality in the human population. In the lower lung, the primary targets for IAV replication are type II alveolar epithelial cells (AECII), which are increasingly recognized for their immunological potential. So far, little is known about their reaction to IAV and their contribution to respiratory antiviral immunity *in vivo*. Therefore, we characterized the AECII response during early IAV infection by analyzing transcriptional regulation in cells sorted from the lungs of infected mice. We detected rapid and extensive regulation of gene expression in AECII following *in vivo* IAV infection. The comparison to transcriptional regulation in lung tissue revealed a strong contribution of AECII to the respiratory response. IAV infection triggered the expression of a plethora of antiviral factors and immune mediators in AECII with a high prevalence for interferon-stimulated genes. Functional pathway analyses revealed high activity in pathogen recognition, immune cell recruitment, and antigen presentation. Ultimately, our analyses of transcriptional regulation in AECII and lung tissue as well as interferon I/III levels and cell recruitment indicated AECII to integrate signals provided by direct pathogen recognition and surrounding cells. *Ex vivo* analysis of AECII proved a powerful tool to increase our understanding of their role in respiratory immune responses, and our results clearly show that AECII need to be considered a part of the surveillance and effector system of the lower respiratory tract.**

IMPORTANCE **In order to confront the health hazard posed by IAV, we need to complete our understanding of its pathogenesis. AECII are primary targets for IAV replication in the lung, and while we are beginning to understand their importance for respiratory immunity, the *in vivo* AECII response during IAV infection has not been analyzed. In contrast to studies addressing the response of AECII infected with IAV *ex vivo*, we have performed detailed gene transcriptional profiling of AECII isolated from the lungs of infected mice. Thereby, we have identified an exceptionally rapid and versatile response to IAV infection that is shaped by pathogen-derived as well as microenvironment-derived signals and aims at the induction of antiviral measures and the recruitment and activation of immune cells. In conclusion, our study presents AECII as active players in antiviral defense *in vivo* that need to be considered part of the sentinel and effector immune system of the lung.**

Received 15 March 2016 **Accepted** 30 March 2016 **Published** 3 May 2016

Citation Stegemann-Koniszewski S, Jeron A, Gereke M, Geffers R, Kröger A, Gunzer M, Bruder D. 2016. Alveolar type II epithelial cells contribute to the anti-influenza A virus response in the lung by integrating pathogen- and microenvironment-derived signals. mBio 7(3):e00276-16. doi:10.1128/mBio.00276-16.

Editor Michael G. Katze, University of Washington

Address correspondence to S. Stegemann-Koniszewski, sabine.stegemann-koniszewski@helmholtz-hzi.de.

Influenza A virus (IAV) still poses a serious threat to human health, and a detailed understanding of IAV pathogenesis is essential to adequately confront this hazard. IAV infections are primarily restricted to the respiratory tract, where epithelial cells, alveolar macrophages (AM), and dendritic cells (DC) trigger the first innate responses (1). IAV bears ligands for several pathogen recognition receptors (PRR), and the main triggered PRR are Toll-like receptor 3 (TLR3) and TLR7 as well as RIG-I, MDA5, and the NLRP3 inflammasome (1). These are engaged in the antiviral response in a cell-type-specific manner (2, 3). Via partly redundant signaling pathways, PRR ligation leads to the activation of effector mechanisms comprised of type I/III interferons (IFNs), inflammatory mediators, antimicrobial effectors, and signals inducing adaptive immunity. In general, viral infections are marked by the strong release of type I interferons. These trigger the expression of a multitude of interferon-stimulated genes (ISG) through the ubiquitously expressed IFN-α/β receptor (IFNAR) (2). ISG expression is also induced through IFN-λ (IFN III), which is released during IAV infection and is sensed through the interleukin-28 (IL-28) receptor α (IL-28Rα) primarily expressed by epithelial cells of the respiratory tract and gut (4).

In the lower respiratory tract, the lining epithelium is comprised of alveolar type I and type II epithelial cells (AECI and AECII, respectively), and at this site, AECII are the main target

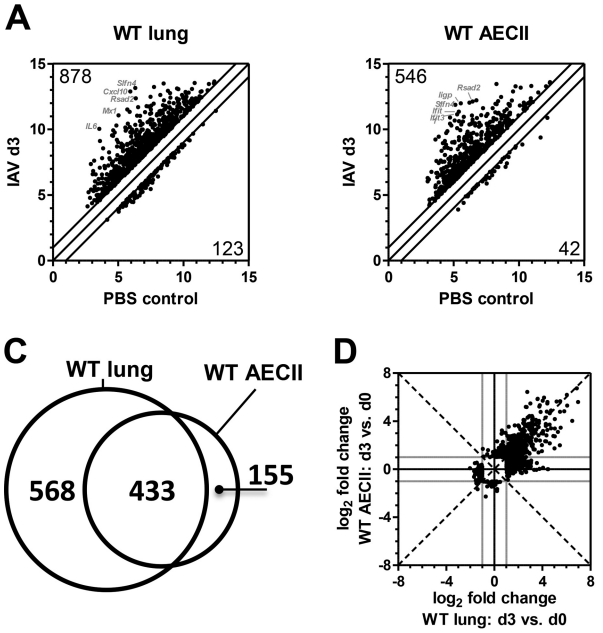

B

Name	FC AECII	FC lung
Slfn4	107.0	115.7
Iigp1	86.5	6.6
Rsad2	73.3	65.2
Ifit1	62.1	17.6
Ifit3	58.4	12.1
Ly6i	57.3	12.0
Ifi44	52.2	16.2
Ms4a4c	49.6	36.2
Cxcl10	48.1	125.5
Gm14446	48.0	21.4
Isg15	44.4	21.1
Ifit2	40.4	13.8
Mx1	39.4	66.2
Oasl2	37.4	13.4
Gbp3	36.6	6.1
Ifi27l2a	36.2	6.4
Cxcl5	29.7	26.4
Zbp1	27.8	20.5
Cxcl9	27.5	44.0
Ddx60	27.3	14.4

FIG 1 Respiratory IAV infection triggers AECII-specific transcriptional regulation. Mice were infected with IAV or treated with PBS and sacrificed 3 days later. Total RNA from whole lungs ($n = 3$ mice for each condition) and sorted AECII ($n = 2$ individual samples for each condition; 5 mice per sample) was subjected to microarray analysis. Data were analyzed by comparing IAV-infected with uninfected control samples. (A) Scatter plots of regulated transcripts with a fold change of $\geq \pm 2$ (threshold represented by the diagonal lines). Data represent normalized $\log_2$ signal intensities (averaged over replicates). The number of up-/downregulated transcripts and the gene symbols of the top 5 upregulated transcripts are indicated. (B) List of the 20 most intensely upregulated transcripts in AECII with fold change values for AECII and lung. (C) Comparison of the transcripts identified in panel A with respect to regulation in lung and/or AECII. (D) Scatter plot showing absolute $\log_2$ fold changes over the respective PBS controls of the transcripts differentially expressed in AECII and/or lung tissue. The dashed bisecting lines indicate equal fold changes. Gray lines indicate the fold change threshold of ± 2.

cells for IAV replication (5, 6). AECII cover about 5% of the alveolar surface, while they comprise about 60% of the alveolar lining cells and 15% of the parenchymal cells (7). Until recently, the secretion of surfactant, the maintenance of the mechanical barrier, and the provision of constitutive antimicrobial defense were conceived as their main functions (7, 8). Beyond these, we are only beginning to understand the potential of AECII to regulate respiratory immune responses in autoimmunity and infection (9–12).

Since AECII are primary targets for viral replication in the lower lung and actively contribute to pulmonary immunity, it is likely that they influence efficient host responses directed at IAV. A number of studies have addressed the response of AECII to IAV *in vitro* and showed them to express functional PRR and to produce cytokines and chemokines (13–17). The nature and the relevance of the AECII response to IAV, however, lack ultimate clarification, as these studies were performed using cell lines or primary cells infected in culture. Little is known about the AECII response to IAV infection *in vivo* and how this contributes to the respiratory immune reaction. To overcome these limitations, we characterized the *in vivo* response of AECII to IAV infection by analyzing primary AECII from the lungs of infected mice.

RESULTS

IAV infection triggers AECII-specific transcriptional regulation *in vivo*. We have previously optimized our IAV infection model for the isolation of pure and viable AECII that express increasing amounts of viral protein over the first days of infection (9, 18). In this model of lethal IAV infection, mice rapidly lose weight, the virus replicates efficiently in the lungs, and high copy numbers of the viral genome are detected in the isolated AECII (see Fig. S1 in the supplemental material). Typically, inflammatory mediators and immune cell recruitment to the respiratory tract are induced by day 3 postinfection (19), and we analyzed transcriptional regulation in AECII and lung tissue at this time point. For AECII, two independent microarray experiments were conducted for each condition and the material for each independent experiment was pooled from five infected animals. For lung tissue, three independent microarrays were performed for each condition and each array represents an independent animal. Fold change (FC) values of 2 or more over controls were considered indicative of up- or downregulation. In lung tissue, 878 transcripts were upregulated and 123 were downregulated following IAV infection. Extensive transcriptional regulation was also detected in AECII, with 546 upregulated and 42 downregulated transcripts (Fig. 1A). In the lung, the 5 most intensely upregulated transcripts were interleukin-6 (IL-6) (FC = 90), CXCL10, and the IFN-induced proteins Mx1 and Rsad2 as well as Slfn4, which has been suggested to be IFN I inducible (20). There was an overlap with AECII, where Rsad2 and Slfn4, along with the IFN-induced proteins Ifit1, Ifit3, and Iigp1, were among the top 5 most regulated transcripts, indicating a prominent role for IFNs in the AECII response (Fig. 1B). The intense upregulation of CXCL5, CXCL9, and CXCL10 (Fig. 1B) in AECII as well as the large overlap of the transcripts found regulated in either lungs or AECII (Fig. 1C) pointed at a strong potential of AECII to contribute to respiratory immunity. In order to confirm the AECII transcriptional regulation following *in vivo* IAV infection detected by the microarray analyses, the expression of a selection of these transcripts was an-

alyzed by quantitative real-time PCR. Indeed, this approach confirmed the significant upregulation of *CXCL5*, *CXCL10*, *IFIT2*, *IRF7*, *MX2*, and *USP18* (see Fig. S2). Overall, the detection of AECII-specific transcripts showed that AECII most likely serve cell-type-specific functions. These transcripts were associated with Gene Ontology (GO) terms such as defense response (Bonferroni corrected *P* value, 2.8×10^{-12}), innate immune response (corrected *P* value, 0.00013), and cytokine production (corrected *P* value, 0.00077). The quality, i.e., whether up- or downregulation occurred, of transcriptional regulation in AECII and lung tissue was not changed between the two sample sets (Fig. 1D). Overall, these results clearly demonstrated that AECII strongly react to IAV infection *in vivo* and hold strong potential to contribute to the respiratory immune response. To characterize this contribution in greater detail, we performed AECII transcriptional analyses over the early course of infection.

Early transcriptional regulation in AECII follows distinct kinetics. Over the first 3 days postinfection, the number of transcripts differentially regulated in AECII strongly increased and the number of downregulated transcripts was considerably lower than the number of those upregulated. This suggested that AECII were increasingly stimulated over time and that activation rather than suppression of gene transcription dictated their response (Fig. 2A). k-means clustering was performed (Fig. 2B to D), and the resulting clusters included transcripts upregulated exclusively only on day 1, 2, or 3 and transcripts downregulated over time. Most differentially expressed transcripts were upregulated on day 3 postinfection, and these further segregated into transcripts (i) slightly upregulated on day 1, (ii) slightly upregulated on days 1 and 2, and (iii) slightly upregulated from day 2 onward (Fig. 2C and D). As IAV infection induces the rapid release of IFN I/III, we assessed the prevalence of ISG within the clusters using the Interferome v2.01 database (21). By far, the highest proportion of ISG was present in clusters 6 and 7, pointing at a strong and progressive AECII response to IFN I and/or IFN III (Fig. 2E).

TLR7 deficiency alters the regulation of gene expression in AECII. We hypothesized that the host relies on IAV-sensing PRR in order to mount a full AECII response and analyzed transcriptional regulation in lungs and AECII of TLR7-knockout (TLR7ko) mice. On day 3 post-IAV infection, considerable transcriptional regulation was detected (see Fig. S3 in the supplemental material). Over time, AECII were increasingly activated also in TLR7ko mice (Fig. 3A). However, the number of upregulated transcripts was clearly reduced in comparison to wild-type (WT) AECII (Fig. 3B), whereas the comparison of gene transcription levels in AECII isolated from uninfected WT and TLR7ko mice did not yield differences in baseline expression (see Fig. S3 in the supplemental material). As there was a large overlap with the transcripts regulated in the WT, TLR7ko AECII did not harbor an independent gene expression profile (Fig. 3C). The 90 transcripts exclusively regulated in TLR7ko AECII were not significantly associated with any annotated Gene Ontology (GO) terms, whereas the transcripts regulated only in WT AECII showed significant association with GO terms such as innate immune response (Bonferroni corrected *P* value, 2.68×10^{-21}), immune effector process (1.38×10^{-18}), and defense response to virus (2.28×10^{-15}). A list of the most intensely regulated of these TLR7-dependent transcripts is provided in Table S1 in the supplemental material. In addition, the fold changes of the vast majority of the transcripts upregulated in both mouse strains were lower in TLR7ko AECII throughout the early course of infection (Fig. 3D). Therefore, the AECII response of TLR7-deficient hosts during IAV infection was blunted regarding both the number of differentially expressed transcripts and the degree of fold change regulation, demonstrating the importance of a single PRR for the full AECII response.

IAV infection triggers transcriptional regulation of a multitude of immunological factors. We performed pathway analyses on the transcripts differentially expressed in AECII on day 3 post-IAV infection using Ingenuity pathway analysis (IPA). The most significantly overrepresented pathways clearly indicated strong immunological activity, as they were involved in pathogen recognition, the induction and shaping of immune responses, and immune cell recruitment (Table 1). Increasing *P* values over time illustrated increasing relevance in the AECII response. These results clearly demonstrated that AECII exert pronounced immunological functions in IAV infection *in vivo*. Of note, the functional pathways overrepresented in the transcripts regulated in TLR7ko AECII were largely identical to those identified for WT AECII (see Table S2 in the supplemental material).

We furthermore evaluated transcriptional regulation of key antiviral and immunological factors within the transcript differentially regulated in AECII. Transcription of several, mainly nucleic acid-sensing PRR was upregulated in AECII in the course of IAV infection (Fig. 4A). Fold change regulation in AECII peaked on day 3 and was similar to or even higher than that detected for whole-lung tissue.

IFIT (IFN-induced protein with tetratricopeptide repeats) 1 to 3, all of which contribute to antiviral defense (22), showed exceptionally strong induction in AECII (Fig. 4B) that by far exceeded that in lung tissue. Interestingly, out of the genes coding for IFN I and IFN III only *Ifnb1* was differentially upregulated in AECII (Fig. 4B). In contrast, also the transcription of interferon regulatory factor 7 (IRF7), which induces IFN and ISG expression (1), was extensively regulated in WT AECII (Fig. 4B).

Also, the transcription of chemokines and cytokines was efficiently induced in AECII, underlining their immunological potential in respiratory infection (Fig. 4C). The extent of upregulation increased over time, and for most cytokines, upregulation was more pronounced in lungs than in AECII. Of note, however, transcription of *Cxcl5*, *Cxcl9*, and *Cxcl10* was upregulated more than 25-fold in AECII and *Cxcl5* and *Ccl5* upregulation in AECII exceeded that in lung tissue.

Next to the secretion of immunological mediators, AECII are capable of presenting antigen on major histocompatibility complex class I (MHC-I) and MHC-II molecules as well as providing costimulation (10, 23–25). Indeed, antigen presentation was among the most significantly enriched pathways in the transcripts differentially expressed in AECII, and the transcriptional regulator of the MHC-I complex NLRC5 (NOD-like receptor family CARD domain-containing 5) as well as Tap1 (transporter associated with antigen processing 1) was upregulated in AECII to a larger extent than in lung tissue (Fig. 4D). Additionally, we detected the upregulation of CD86 as well as H2-DMb2 in AECII following IAV infection.

For the selected factors, transcriptional regulation in TLR7ko AECII showed similar kinetics but in the majority of cases did not reach the magnitude of upregulation observed in WT AECII (see Fig. S4 in the supplemental material). Taken together, AECII reacted to respiratory IAV infection by the differential expression of

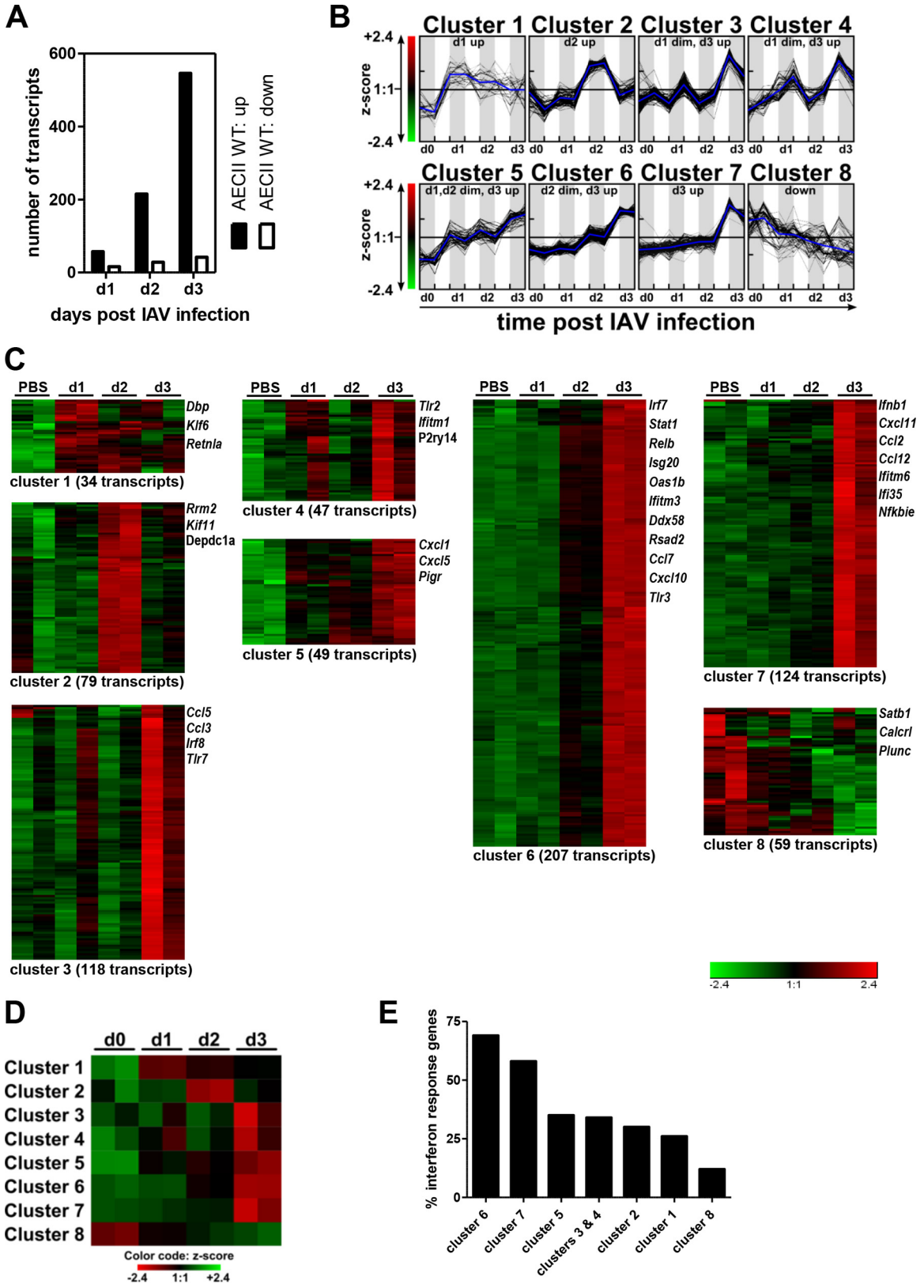

FIG 2 Kinetics of transcriptional regulation in WT AECII in the early course of IAV infection. Mice were infected with IAV and sacrificed 1, 2, or 3 days later. RNA from sorted AECII ($n = 2$ individual samples for each condition; 5 mice per sample) was subjected to microarray analysis. For each time point, microarray data were compared to the uninfected control. (A) The number of transcripts up-/downregulated with a fold change of $\geq \pm 2$ in AECII. (B) k-means cluster analysis of the transcripts differentially regulated with a fold change of $\geq \pm 2$ in AECII on day 1, 2, or 3. Data were transformed into Z scores. Line plots show the

(Continued)

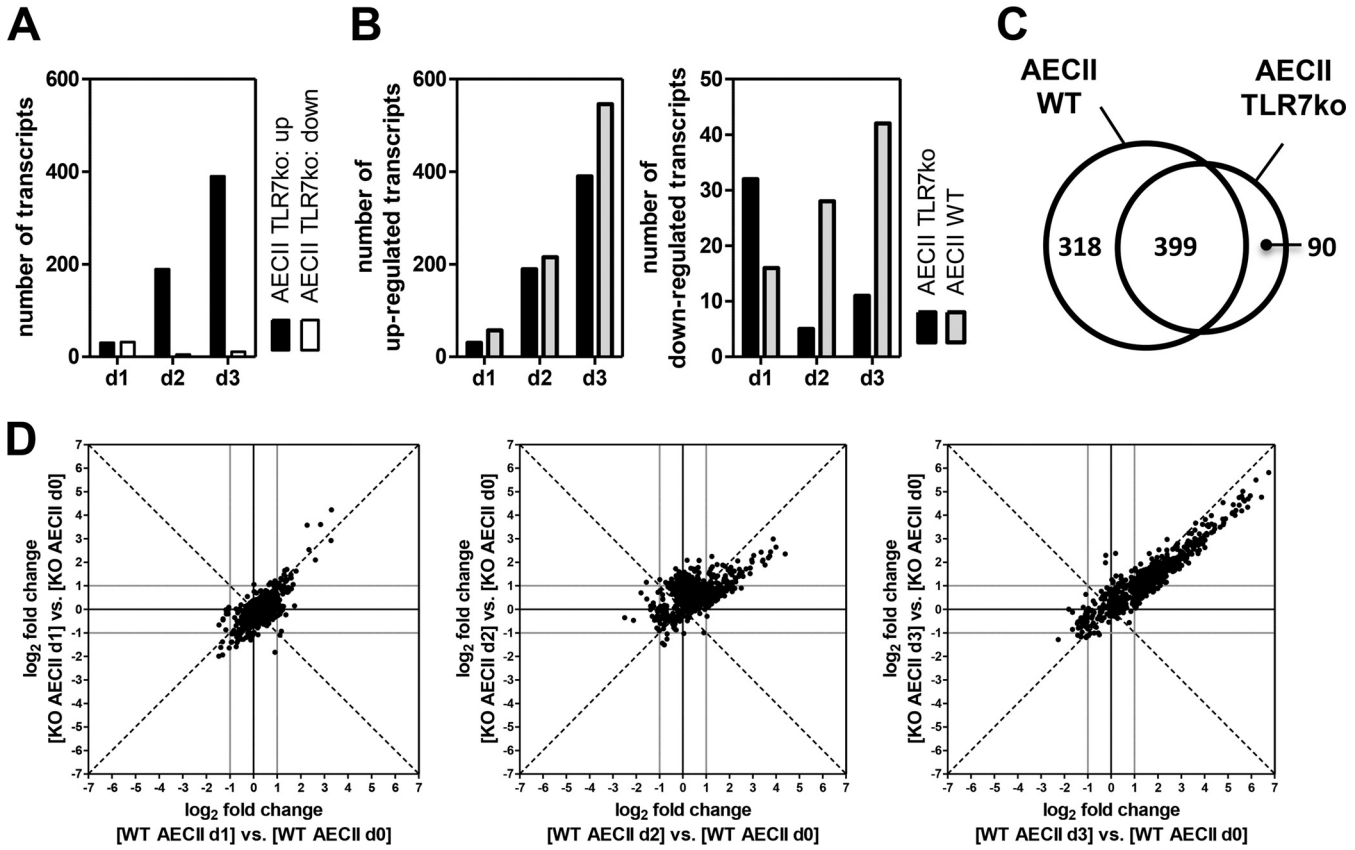

FIG 3 Transcriptional regulation in response to IAV infection is blunted in AECII isolated from TLR7-deficient hosts. Wild-type (WT) and TLR7ko mice were infected with IAV and sacrificed 1, 2, or 3 days postinfection. RNA from sorted AECII ($n = 2$ individual samples per time point; 5 mice per sample) was subjected to microarray analysis. For each time point, microarray data were compared to the respective uninfected control. (A) Number of transcripts up- or downregulated with a fold change of $\geq \pm 2$ in TLR7ko AECII in the course of IAV infection. (B) Comparison between the number of up- and downregulated transcripts in WT and TLR7ko AECII. (C) Venn diagram comparing the transcripts regulated in AECII on day 1, 2, and/or 3 post-IAV infection with regard to their regulation in WT AECII, TLR7ko AECII, or both. (D) Scatter plots displaying the absolute $\log_2$ fold changes of the transcripts regulated more than 2-fold (up or down) in WT and/or TLR7ko AECII on days 1, 2, and/or 3 post-IAV infection. The dashed bisecting lines indicate equal fold changes. Gray lines indicate the fold change threshold of ± 2.

a multitude of molecules involved in the induction and shaping of immune responses, demonstrating their exceptionally high potential to contribute to respiratory immunity *in vivo*.

AECII transcriptional regulation correlates with PMN recruitment and IFN I/III levels. AECII most likely take part in the recruitment of immune effector cells to the respiratory tract. We determined the overall cellularity of bronchoalveolar lavage (BAL) fluid, and a strong and significant increase in cell numbers was detected on day 3 postinfection (Fig. 5A). Since the majority of the chemokines differentially expressed in AECII act as chemoattractants for macrophages and other myeloid cells, mainly polymorphonuclear neutrophils (PMN), we determined the macrophage and PMN populations. In uninfected mice, macrophages were the main cell type present and their relative contribution was significantly reduced by day 3 (Fig. 5B). At the same time, there was a significant increase in the PMN population size and the absolute PMN number (Fig. 5B and C). The kinetics of PMN recruitment and AECII transcriptional regulation of chemokines suggest that AECII contribute to the attraction of innate effectors to the lung. Of note, the blunted transcriptional regulation of chemokines in TLR7-deficient hosts was in line with a delayed recruitment of PMN (see Fig. S5 in the supplemental material).

In order to link ISG induction to interferon levels in the lung, we assessed the levels of bioactive IFN I/III in BAL fluid. A substantial increase in IFN I/III activity was detected on day 2 post-IAV infection, with a significant increase by day 3 (Fig. 5C) which directly correlated with the massive induction of ISG in AECII by day 3 postinfection. Of note, IFN I/III levels were significantly reduced in TLR7-deficient mice (see Fig. S5 in the supplemental material). Taken together, these findings imply a critical role for IFN I/III for the AECII response following IAV infection.

Figure Legend Continued

Z scores of the transcripts of the individual k-means clusters over time (for both replicates per time point). The blue lines indicate the average Z score. (C) Heat map visualization of the Z scores in the individual k-means clusters. The number of transcripts and selected members are indicated for each cluster. (D) Heat map visualization of the average Z score value per column of the k-means clusters. (E) Percent interferon response genes within the individual k-means clusters as determined using the Interferome v2.01 database.

TABLE 1 Functional pathways most significantly overrepresented in the transcripts differentially expressed in AECII[a]

Ranking by *P* value	Canonical pathway	AECII day 1	AECII day 2	AECII day 3
1	Communication between innate and adaptive immune cells	1.53	2.05	20.49
2	Role of pattern recognition receptors in recognition of bacteria and viruses		3.03	19.04
3	Granulocyte adhesion and diapedesis	2.53	3.31	15.44
4	Cross talk between dendritic cells and natural killer cells			14.79
5	Dendritic cell maturation			14.33
6	TREM1 signaling	1.73	2.42	13.79
7	Agranulocyte adhesion and diapedesis	2.44	3.14	12.91
8	Altered T cell and B cell signaling in rheumatoid arthritis			12.79
9	Interferon signaling		4.56	12.64
10	Antigen presentation pathway		2.34	11.66

[a] The 10 pathways most significantly overrepresented in the transcripts differentially regulated in WT AECII on day 3 postinfection are listed. Pathways were ranked by Fisher exact test *P* value. The data columns indicate the $-\log(P \text{ value})$ for overrepresentation of the respective pathways for all microarray data sets (WT AECII; days 1, 2, and 3 postinfection), listing only those values indicating statistical significance ($P < 0.05$).

DISCUSSION

Nearly all of the research that has addressed the response of AECII to IAV was performed in cells infected with the virus *ex vivo* (13–17), whereas *in vivo* studies mostly did not differentiate between different cell types of the epithelium (26).

Our analyses revealed that AECII strongly react to respiratory IAV infection *in vivo*. The response was exceptionally versatile and included differential expression of a plethora of factors associated with antiviral activity and the induction of immune responses. Several antiviral proteins were among the most intensely upregulated transcripts, and the importance of their epithelial expression was highlighted by the finding that fold change induction in AECII often exceeded that in lung tissue. Deficiency in IFITM3, which was upregulated 12-fold in AECII and only 2-fold in lung tissue on day 3 (data not shown), leads to enhanced viral titers and increased mortality in mice, and patients with *IFITM3* mutations exhibit compromised IAV restriction (27). Also, ISG15 and Gbp3 (guanylate-binding protein 3) contribute specifically to the anti-IAV host defense (28, 29). Out of the genes encoding IFN I/III, only *Ifnb1* was upregulated in AECII following *in vivo* IAV infection. This was surprising at first, especially as AECII are described to produce IFN I/III in response to IAV both *in vivo* and *in vitro* (13, 30). However, it has been shown that during *in vivo* IAV infection IFN-β is predominantly produced not by the epithelium but by CD11c-expressing cell populations (31). Furthermore, the depletion of plasmacytoid dendritic cells (pDC) was reported to lead to a significantly diminished IFN I production in the lungs of IAV-infected mice (32). Therefore, we believe that also in our model resident and newly recruited pDC are most likely the main producers of IFN I. This is well in line with the significantly decreased IFN I/III production in TLR7ko mice, as pDC are known to depend on TLR7 (33).

Extensive transcriptional regulation of *CXCL5*, *CXCL9*, and *CXCL10* demonstrated how broadly AECII act on pulmonary host defense. Even though upregulation of most cytokines in lung tissue exceeded that in AECII, upregulation of *CXCL5* and *CCL5* in AECII was stronger than in lung tissue. Blocking of CCL5 in respiratory viral infection reduces the recruitment of $CD4^+$ and $CD8^+$ T cells (34), and AECII are the predominant source of CXCL5 in the lungs of mice treated with lipopolysaccharide (35). Regarding the role of AECII in the recruitment of effector cells, the significantly attenuated PMN recruitment in TLR7ko mice was well in line with the alleviated induction of CXCL5 expression in their AECII. Of note, however, this reduction in PMN recruitment is not necessarily a consequence of the reduced production of chemotactic cytokines only by AECII, as their upregulation was also strongly reduced in whole-lung tissue of TLR7ko mice. Nevertheless, the extensive induction of cytokine and chemokine transcription in AECII pointed at a strong contribution of AECII to the overall lung response to infection *in vivo*.

Next to MHC-I antigen presentation in AECII, there was also evidence for MHC-II presentation and costimulation. In fact, lethal IAV infection induces MHC-II expression on lung epithelial cells (23), and AECII have been observed to present antigen to $CD4^+$ T cells in the context of mycobacterial infection (25). Furthermore, we have previously shown that AECII efficiently present antigen to and activate $CD4^+$ T cells and that they are able to promote the induction of regulatory T cells (10). Therefore, MHC-I and also MHC-II antigen presentation displays strategies for AECII to shape the lower respiratory tract immune response during IAV infection *in vivo*.

A clear and distinct role for TLR7 in survival following IAV infection has so far been demonstrated only in mice expressing functional Mx1, unlike the commonly used laboratory mouse strains (36). We and others have rather found TLR7 to be involved in the fine-tuning of innate and adaptive anti-IAV responses (19, 37, 38), and in our model of respiratory IAV infection, there was no difference in morbidity and mortality between WT and TLR7-deficient hosts (see Fig. S6 in the supplemental material). Nevertheless, we found the AECII response to IAV to be substantially blunted in the absence of TLR7. As both unchanged and clearly diminished IFN I production have been described in TLR7ko mice (19, 39), it was surprising that TLR7 played such a central role in ensuring a robust early IFN response in our model. Most likely, the reduced levels of IFN I/III in the respiratory tract of TLR7ko mice to a large extent accounted for the blunted AECII response in these mice, especially since many of the regulated transcripts were ISG. Of note, the numbers of AECII isolated from WT and TLR7ko animals were similar (see Fig. S6 in the supplemental material). However, TLR7ko mice displayed a reduction in viral load in lung tissue and the isolated AECII (see Fig. S6 in the supplemental material). IAV has previously been described to depend on TLR7 for efficient replication (39), and this reduction in viral load, even though not significant by day 3, was a likely reason for the blunted IFN I/III and in turn the blunted AECII response in TLR7ko mice. We are not able to dissect the interdependence of viral replication, IFN I/III production, and transcriptional regulation in AECII from our data. Silencing of TLR7 and other IAV

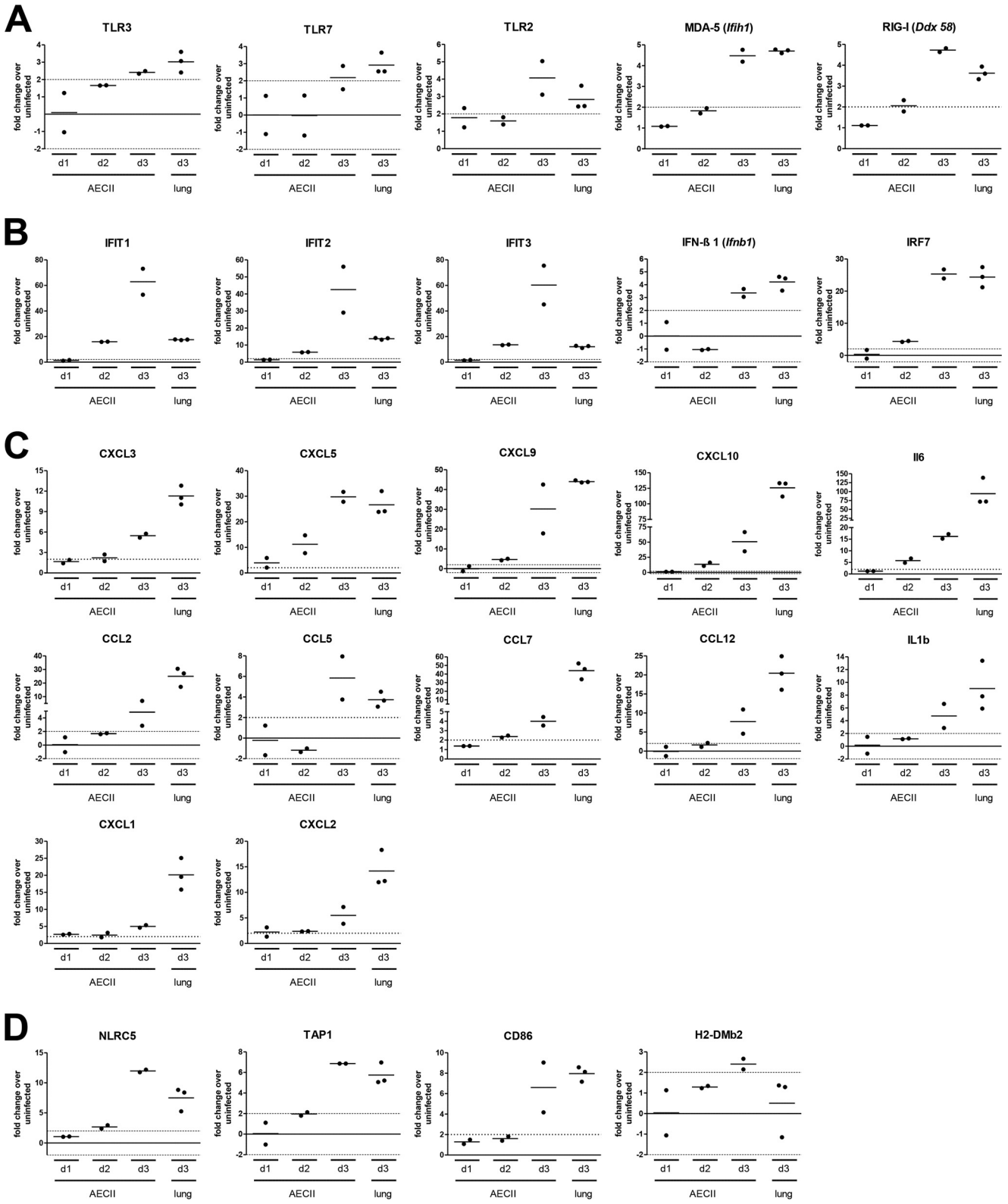

FIG 4 IAV infection triggers the differential expression of a multitude of molecules involved in antimicrobial defense. The graphs depict the fold change regulation of selected transcripts as determined by microarray analysis of WT AECII and lungs isolated at the indicated time points post-IAV infection. Data are shown as the mean and the individual results from two independent replicate microarray experiments (2 independent samples; 5 mice per sample) for AECII and three independent replicate microarray experiments for lung tissue (three independent samples). The transcripts listed are grouped into those encoding pathogen recognition receptors (A), factors associated with the IFN I/III response (B), cytokines and chemokines (C), and factors associated with antigen presentation (D). For each bar graph, the dashed horizontal line indicates a fold change of 2.

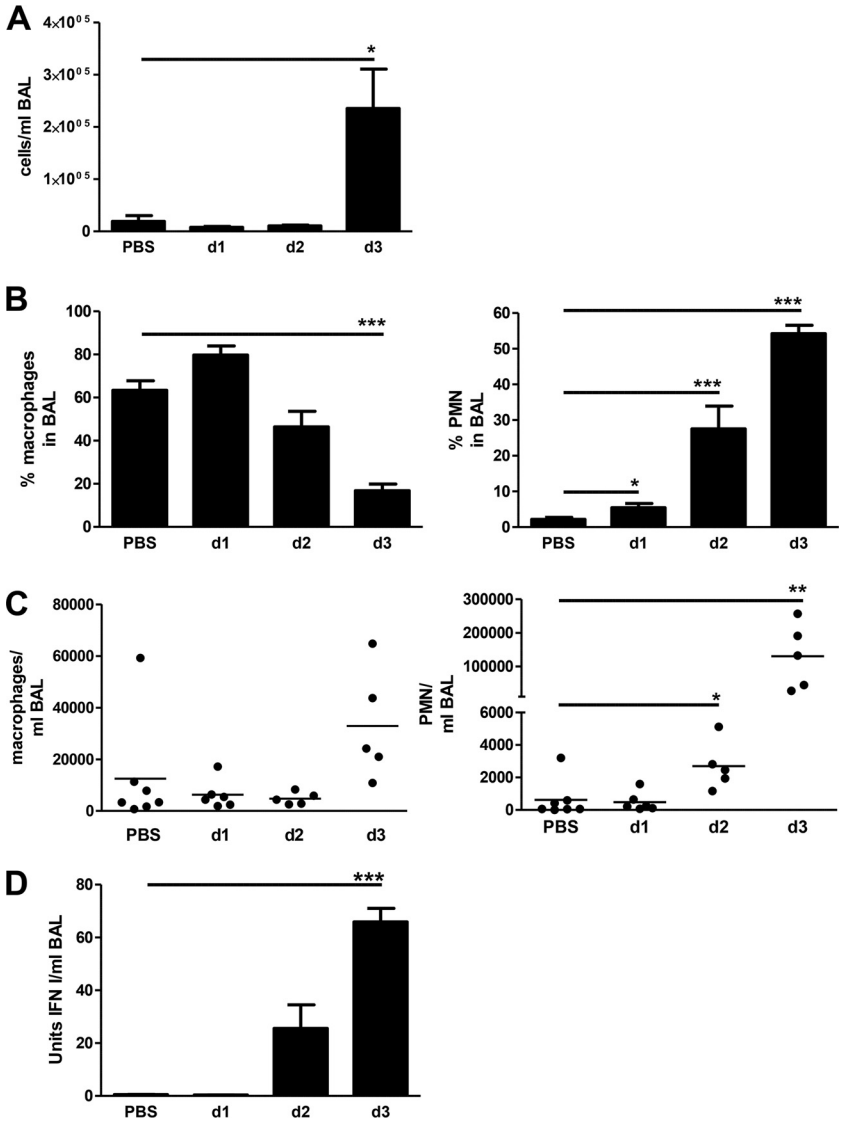

FIG 5 The kinetics of cell recruitment and type I/III interferon levels correlate with AECII transcriptional profiles. WT mice were sacrificed at the indicated time points post-IAV infection. Bronchoalveolar lavage (BAL) fluid cells were counted (A), and the macrophage and polymorphonuclear cell (PMN) populations (B) were assessed by flow cytometry. Cell populations were analyzed by gating on macrophages ($F4/80^+$ cells) within all acquired cells and gating on PMN ($Gr\text{-}1^+/CD11b^+$) within the $F4/80^-$ cell fraction. (C) Cell numbers were calculated from the absolute cell count and percent population for all analyzed individual mice. Data from individual mice and the mean per group are shown. (D) The concentration of bioactive type I IFN in BAL fluid was assessed using IFN I/III-sensitive reporter cells and an IFN-β standard. Data are shown as means ± standard errors of the means or as individual mice and mean per group. All data are compiled from $n \geq 5$ mice out of at least two independent experiments. Groups were compared by unpaired, two-sided *t* test (*P* values: *, <0.05; **, <0.005; ***, <0.001).

sensors such as RIG-I specifically in AECII will be essential to shed light on this issue. Nevertheless, the high number of ISG triggered and the correlation between the AECII response and IFN I/III levels in the lung clearly showed that AECII react to their specific microenvironment *in vivo*. In addition to our findings, cell culture studies have shown that pretreatment of AECII with tumor necrosis factor alpha (TNF-α) and IFN-α greatly enhanced their cytokine and chemokine response to IAV (16). Also, IL-17A and TNF-α synergistically act on CXCL5 expression by AECII *in vitro* and *in vivo* (40).

Ultimately, the detailed contributions and interplay of pathogen recognition and the signals provided by the microenvironment remain a central question for our understanding of AECII activation *in vivo*. Dynamic PRR expression patterns in response to IAV have been observed for AECII (41), and moreover, they respond directly to the virus through various TLR (30, 42). In our study, the exceptionally rapid induction of gene expressional changes and the transcriptional upregulation of nucleic acid-sensing PRR in the course of the infection suggested a direct sensing of the virus by AECII also *in vivo*. Many of the transcripts differentially expressed in AECII are typically triggered by PRR ligation and activation of the NF-κB pathway, and the functional pathway Role of Pattern Recognition Receptors in Recognition of Bacteria and Viruses was the second most significantly overrepresented pathway. Therefore, we propose a model in which the rapid and versatile *in vivo* AECII response following IAV infection is

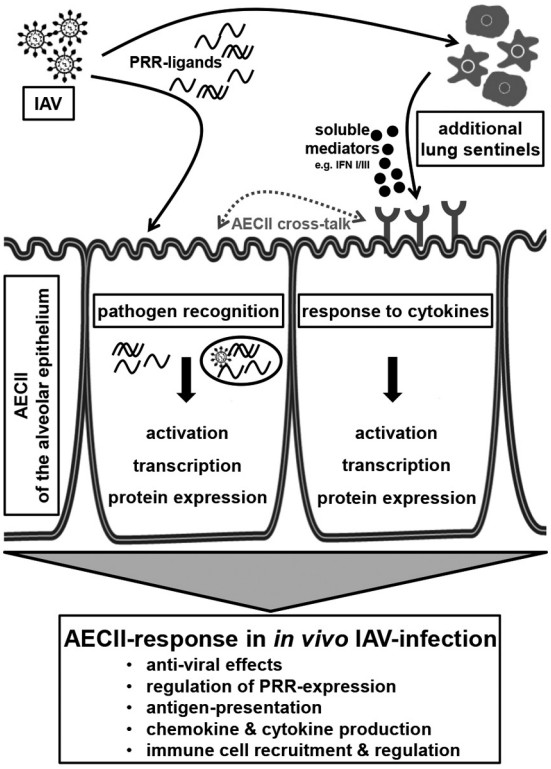

FIG 6 Integrative model of the contribution of AECII to lower respiratory tract anti-IAV responses. The analysis of transcriptional regulation in AECII isolated from infected mice revealed their rapid and versatile immunological response to IAV infection *in vivo*. Based on our results, we propose that AECII integrate signals from a direct interaction with the pathogen with signals provided through cytokines released by additional sentinel cells in order to mount this response.

triggered by PRR ligation as well as soluble mediators (Fig. 6). Our results show that the *in vivo* AECII response aims at the inhibition of viral replication and the recruitment and activation of effector cells. Furthermore, we highlight the need to study AECII within their microenvironment to fully characterize their response to pathogens and their role in the local immune system.

MATERIALS AND METHODS

Mice. C57BL/6 mice were purchased from Harlan, and TLR7ko mice (43) (provided by S. Bauer) were bred at the Helmholtz Centre for Infection Research. Eight- to 12-week-old mice were used. Control groups were age and sex matched. All animal experimental procedures were approved by the local government agency (Nds. Landesamt für Verbraucherschutz und Lebensmittelsicherheit, file no. 33.9-42502-04-11/0443).

Influenza A virus infection. Madin-Darby canine kidney (MDCK) cell-derived IAV PR8/A/34(H1N1) was obtained as described previously (19). Following intraperitoneal injection of ketamine-xylazine, mice were intranasally infected with $10^{1.8}$ 50% tissue culture infective doses ($TCID_{50}$) in 40 μl phosphate-buffered saline (PBS).

AECII isolation. AECII isolation was performed as described previously (9, 18). Briefly, lungs were perfused and instilled with dispase (5,000 caseinolytic units/100 ml; BD Biosciences) followed by 1% low-melting-point agarose. Excised lungs were incubated in dispase for 45 min. The tissue was disintegrated and incubated for 10 min in Dulbecco's Modified Eagle Medium (DMEM) (Gibco, Life Technologies) supplemented with 650 Kunitz units of bovine DNase I (Sigma-Aldrich) and anti-CD16/32 (2.4G2). Cell suspensions were filtered, and crude cell suspensions from separate mice were pooled. Cells were stained using antibodies for CD16/32 (clone 93), F4/80 (BM8), CD11b (M1/70), CD11c (N418), CD19 (1D3), and CD45 (30-F11). AECII were isolated by sorting for granular sideward $scatter^{high}$ cells negative for the antibody staining using a BD FACSAria instrument.

Expression microarray analysis. RNA was isolated from 1×10^6 AECII/sample. For lung tissue, lungs were perfused with PBS, excised, homogenized in RLT buffer (Qiagen), and centrifuged. RNA was isolated from the supernatant using the RNeasy minikit (Qiagen). DNA was digested using the RNase-free DNase set (Qiagen). RNA integrity was tested using the Agilent 2100 Bioanalyzer (Agilent Technologies) with the RNA 6000 Nano/Pico kit (Agilent Technologies). Synthesis and fragmentation of labeled cRNA were performed using the GeneChip 3′ IVT Express kit (Affymetrix). For AECII, two independent microarray experiments were conducted for each condition and the material for each independent experiment was pooled from five infected animals. For lung tissue, three independent microarrays were performed for each condition and each array represents an independent animal. All samples were hybridized to GeneChip Mouse Genome 430 2.0 microarrays (Affymetrix) and stained according to the manufacturer's recommendations. Microarrays were scanned with an Affymetrix GCS 3000 scanner running with GCOS v1.1.1 software. Every analyzed gene is represented by 16 independent probe pairs which establish the basis for the statistical evaluation. Therefore, only reproducibly regulated genes are included in the analysis.

Data analysis. Microarray data were analyzed using GeneSpring GX (Agilent Technologies). The data were summarized, $\log_2$ transformed, and normalized with the Robust Multi-array Analysis (RMA) algorithm. To exclude probe sets with consistently low signal intensities in all microarrays performed, only probe sets with signal intensities above the 20th percentile in at least one of all the performed microarrays were retained. The signal intensities of the replicate arrays from lungs and AECII were averaged, and fold changes were calculated in reference to respective uninfected lung/AECII controls. With respect to the analyzed sample material, in total 8 comparative conditions were considered for fold change calculation, i.e., [IAV-WT-lung-d3] versus [PBS-WT-lung-d0], [IAV-TLR7ko-lung-d3] versus [PBS-TLR7ko-lung-d0], [IAV-WT-AECII-d1] versus [PBS-WT-AECII-d0], [IAV-WT-AECII-d2] versus [PBS-WT-AECII-d0], [IAV-WT-AECII-d3] versus [PBS-WT-AECII-d0], [IAV-TLR7ko-AECII-d1] versus [PBS-TLR7ko-AECII-d0], [IAV-TLR7ko-AECII-d2] versus [PBS-TLR7ko-AECII-d0], and [IAV-TLR7ko-AECII-d3] versus [PBS-TLR7ko-AECII-d0]. Depending on the type of the biological question, only certain combinations of the 8 comparative conditions were considered, i.e., comparison of lungs versus AECII in WT mice; comparison of lungs versus AECII in TLR7ko mice; comparison of WT AECII d1, d2, and d3 versus d0; and comparison of TLR7ko AECII d1, d2, and d3 versus d0. In each analysis, a fold change of $> \pm 2$ in at least one out of the regarded conditions was considered indicative for a gene to be up- or downregulated. Fold change calculation considering all 8 comparative conditions results in 1,815 regulated probe sets. Signal intensities of regulated genes were further analyzed by k-means clustering, using the individual microarray replicates and using the Genesis software 1.7.3 (44) following Z score transformation (45). Gene Ontology and pathway analysis was performed with Qiagen's Ingenuity pathway analysis tool (Ingenuity Systems).

Detection of IFN I/III in bronchoalveolar lavage (BAL) fluid. Lungs were flushed with 1 ml saline through the trachea, and samples were spun at $10{,}000 \times g$. To determine the amount of IFN I/III, IFN-sensitive epithelial cells from Mx2-Luc reporter mice were treated with the supernatant as described previously (46). A standard curve for the calculation of IFN concentrations was obtained by treating cells with serial dilutions of IFN-β.

Flow cytometric analysis. Cells were collected from BAL fluid, were incubated with a CD16/CD36 (2.4G2) antibody, and stained for CD11b (M1/70), Gr-1 (RB6-8C5), and F4/80 (BM8). Data were acquired using a BD LSRFortessa cell analyzer and analyzed using FlowJo (Tree Star).

Microarray data accession number. Microarray data were deposited in NCBI's Gene Expression Omnibus and are accessible through the GEO series accession number GSE57008.

SUPPLEMENTAL MATERIAL

Supplemental material for this article may be found at http://mbio.asm.org/lookup/suppl/doi:10.1128/mBio.00276-16/-/DCSupplemental.

Figure S1, PDF file, 0.4 MB.
Figure S2, PDF file, 0.3 MB.
Figure S3, PDF file, 0.4 MB.
Figure S4, PDF file, 0.2 MB.
Figure S5, PDF file, 0.2 MB.
Figure S6, PDF file, 0.2 MB.
Table S1, PDF file, 0.02 MB.
Table S2, PDF file, 0.02 MB.

ACKNOWLEDGMENTS

This work was supported by the German Research Foundation (BR2221/1-1 to D. Bruder and GU769/5-1 to M. Gunzer) and the Helmholtz Association (HGF) (President's Initiative and Networking Fund W2/W3-029 to D. Bruder).

We thank S. Akira (Osaka University) for permission to obtain TLR7ko mice; L. Gröbe and M. Höxter (Helmholtz Centre for Infection Research) for cell sorting; and P. Hagendorff, S. Kaser, S. Prettin, T. Hirsch, and M. Grashoff (Helmholtz Centre for Infection Research) and F. Ewert (Otto-von-Guericke University Magdeburg) for technical assistance.

FUNDING INFORMATION

This work, including the efforts of Dunja Bruder and Matthias Gunzer, was funded by Deutsche Forschungsgemeinschaft (DFG) (BR2221/1-1 and GU769/5-1). This work, including the efforts of Dunja Bruder, was funded by Helmholtz-Gemeinschaft (Helmholtz Association) (W2/W3-029).

REFERENCES

1. **Iwasaki A, Pillai PS.** 2014. Innate immunity to influenza virus infection. Nat Rev Immunol **14:**315–328. http://dx.doi.org/10.1038/nri3665.
2. **Kato H, Sato S, Yoneyama M, Yamamoto M, Uematsu S, Matsui K, Tsujimura T, Takeda K, Fujita T, Takeuchi O, Akira S.** 2005. Cell type-specific involvement of RIG-I in antiviral response. Immunity **23:**19–28. http://dx.doi.org/10.1016/j.immuni.2005.04.010.
3. **Kato H, Takeuchi O, Sato S, Yoneyama M, Yamamoto M, Matsui K, Uematsu S, Jung A, Kawai T, Ishii KJ, Yamaguchi O, Otsu K, Tsujimura T, Koh CS, Reis e Sousa C, Matsuura Y, Fujita T, Akira S.** 2006. Differential roles of MDA5 and RIG-I helicases in the recognition of RNA viruses. Nature **441:**101–105. http://dx.doi.org/10.1038/nature04734.
4. **Mordstein M, Kochs G, Dumoutier L, Renauld JC, Paludan SR, Klucher K, Staeheli P.** 2008. Interferon-lambda contributes to innate immunity of mice against influenza A virus but not against hepatotropic viruses. PLoS Pathog **4:**e1000151. http://dx.doi.org/10.1371/journal.ppat.1000151.
5. **Koerner I, Matrosovich MN, Haller O, Staeheli P, Kochs G.** 2012. Altered receptor specificity and fusion activity of the haemagglutinin contribute to high virulence of a mouse-adapted influenza A virus. J Gen Virol **93:**970–979. http://dx.doi.org/10.1099/vir.0.035782-0.
6. **Weinheimer VK, Becher A, Tönnies M, Holland G, Knepper J, Bauer TT, Schneider P, Neudecker J, Rückert JC, Szymanski K, Temmesfeld-Wollbrueck B, Gruber AD, Bannert N, Suttorp N, Hippenstiel S, Wolff T, Hocke AC.** 2012. Influenza A viruses target type II pneumocytes in the human lung. J Infect Dis **206:**1685–1694. http://dx.doi.org/10.1093/infdis/jis455.
7. **Fehrenbach H.** 2001. Alveolar epithelial type II cell: defender of the alveolus revisited. Respir Res **2:**33–46. http://dx.doi.org/10.1186/rr36.
8. **Mason RJ.** 2006. Biology of alveolar type II cells. Respirology **11**(Suppl): S12–S15. http://dx.doi.org/10.1111/j.1440-1843.2006.00800.x.
9. **Gereke M, Gröbe L, Prettin S, Kasper M, Deppenmeier S, Gruber AD, Enelow RI, Buer J, Bruder D.** 2007. Phenotypic alterations in type II alveolar epithelial cells in CD4$^+$ T cell mediated lung inflammation. Respir Res **8:**47. http://dx.doi.org/10.1186/1465-9921-8-47.
10. **Gereke M, Jung S, Buer J, Bruder D.** 2009. Alveolar type II epithelial cells present antigen to CD4(+) T cells and induce Foxp3(+) regulatory T cells. Am J Respir Crit Care Med **179:**344–355. http://dx.doi.org/10.1164/rccm.200804-592OC.
11. **Sato K, Tomioka H, Shimizu T, Gonda T, Ota F, Sano C.** 2002. Type II alveolar cells play roles in macrophage-mediated host innate resistance to pulmonary mycobacterial infections by producing proinflammatory cytokines. J Infect Dis **185:**1139–1147. http://dx.doi.org/10.1086/340040.
12. **Unkel B, Hoegner K, Clausen BE, Lewe-Schlosser P, Bodner J, Gattenloehner S, Janssen H, Seeger W, Lohmeyer J, Herold S.** 2012. Alveolar epithelial cells orchestrate DC function in murine viral pneumonia. J Clin Invest **122:**3652–3664. http://dx.doi.org/10.1172/JCI62139.
13. **Crotta S, Davidson S, Mahlakoiv T, Desmet CJ, Buckwalter MR, Albert ML, Staeheli P, Wack A.** 2013. Type I and type III interferons drive redundant amplification loops to induce a transcriptional signature in influenza-infected airway epithelia. PLoS Pathog **9:**e1003773. http://dx.doi.org/10.1371/journal.ppat.1003773.
14. **Gan H, Hao Q, Idell S, Tang H.** 2015. Transcription factor Runx3 is induced by influenza A virus and double-strand RNA and mediates airway epithelial cell apoptosis. Sci Rep **5:**17916. http://dx.doi.org/10.1038/srep17916.
15. **Ito Y, Correll K, Zemans RL, Leslie CC, Murphy RC, Mason RJ.** 2015. Influenza induces IL-8 and GM-CSF secretion by human alveolar epithelial cells through HGF/c-Met and TGF-alpha/EGFR signaling. Am J Physiol Lung Cell Mol Physiol **308:**L1178–L1188. http://dx.doi.org/10.1152/ajplung.00290.2014.
16. **Veckman V, Osterlund P, Fagerlund R, Melén K, Matikainen S, Julkunen I.** 2006. TNF-alpha and IFN-alpha enhance influenza-A-virus-induced chemokine gene expression in human A549 lung epithelial cells. Virology **345:**96–104. http://dx.doi.org/10.1016/j.virol.2005.09.043.
17. **Yu WC, Chan RW, Wang J, Travanty EA, Nicholls JM, Peiris JS, Mason RJ, Chan MC.** 2011. Viral replication and innate host responses in primary human alveolar epithelial cells and alveolar macrophages infected with influenza H5N1 and H1N1 viruses. J Virol **85:**6844–6855. http://dx.doi.org/10.1128/JVI.02200-10.
18. **Gereke M, Autengruber A, Gröbe L, Jeron A, Bruder D, Stegemann-Koniszewski S.** 2012. Flow cytometric isolation of primary murine type II alveolar epithelial cells for functional and molecular studies. J Vis Exp **70:**4322. http://dx.doi.org/10.3791/4322.
19. **Stegemann-Koniszewski S, Gereke M, Orrskog S, Lienenklaus S, Pasche B, Bader SR, Gruber AD, Akira S, Weiss S, Henriques-Normark B, Bruder D, Gunzer M.** 2013. TLR7 contributes to the rapid progression but not to the overall fatal outcome of secondary pneumococcal disease following influenza A virus infection. J Innate Immun **5:**84–96. http://dx.doi.org/10.1159/000345112.
20. **Katsoulidis E, Carayol N, Woodard J, Konieczna I, Majchrzak-Kita B, Jordan A, Sassano A, Eklund EA, Fish EN, Platanias LC.** 2009. Role of Schlafen 2 (SLFN2) in the generation of interferon alpha-induced growth inhibitory responses. J Biol Chem **284:**25051–25064. http://dx.doi.org/10.1074/jbc.M109.030445.
21. **Rusinova I, Forster S, Yu S, Kannan A, Masse M, Cumming H, Chapman R, Hertzog PJ.** 2013. Interferome v2.0: an updated database of annotated interferon-regulated genes. Nucleic Acids Res **41:**D1040–D1046. http://dx.doi.org/10.1093/nar/gks1215.
22. **Diamond MS, Farzan M.** 2013. The broad-spectrum antiviral functions of IFIT and IFITM proteins. Nat Rev Immunol **13:**46–57. http://dx.doi.org/10.1038/nri3344.
23. **Brown DM, Lee S, Garcia-Hernandez MDLL, Swain SL.** 2012. Multifunctional CD4 cells expressing gamma interferon and perforin mediate protection against lethal influenza virus infection. J Virol **86:**6792–6803. http://dx.doi.org/10.1128/JVI.07172-11.
24. **Corbière V, Dirix V, Norrenberg S, Cappello M, Remmelink M, Mascart F.** 2011. Phenotypic characteristics of human type II alveolar epithelial cells suitable for antigen presentation to T lymphocytes. Respir Res **12:**15. http://dx.doi.org/10.1186/1465-9921-12-15.
25. **Debbabi H, Ghosh S, Kamath AB, Alt J, Demello DE, Dunsmore S, Behar SM.** 2005. Primary type II alveolar epithelial cells present microbial antigens to antigen-specific CD4$^+$ T cells. Am J Physiol Lung Cell Mol Physiol **289:**L274–L279. http://dx.doi.org/10.1152/ajplung.00004.2005.
26. **Brandes M, Klauschen F, Kuchen S, Germain RN.** 2013. A systems analysis identifies a feedforward inflammatory circuit leading to lethal influenza infection. Cell **154:**197–212. http://dx.doi.org/10.1016/j.cell.2013.06.013.

27. **Everitt AR, Clare S, Pertel T, John SP, Wash RS, Smith SE, Chin CR, Feeley EM, Sims JS, Adams DJ, Wise HM, Kane L, Goulding D, Digard P, Anttila V, Baillie JK, Walsh TS, Hume DA, Palotie A, Xue Y.** 2012. IFITM3 restricts the morbidity and mortality associated with influenza. Nature **484:**519–523. http://dx.doi.org/10.1038/nature10921.
28. **Lenschow DJ, Lai C, Frias-Staheli N, Giannakopoulos NV, Lutz A, Wolff T, Osiak A, Levine B, Schmidt RE, García-Sastre A, Leib DA, Pekosz A, Knobeloch KP, Horak I, Virgin HW.** 2007. IFN-stimulated gene 15 functions as a critical antiviral molecule against influenza, herpes, and Sindbis viruses. Proc Natl Acad Sci U S A **104:**1371–1376. http://dx.doi.org/10.1073/pnas.0607038104.
29. **Nordmann A, Wixler L, Boergeling Y, Wixler V, Ludwig S.** 2012. A new splice variant of the human guanylate-binding protein 3 mediates anti-influenza activity through inhibition of viral transcription and replication. FASEB J **26:**1290–1300. http://dx.doi.org/10.1096/fj.11-189886.
30. **Ioannidis I, Ye F, McNally B, Willette M, Flaño E.** 2013. Toll-like receptor expression and induction of type I and type III interferons in primary airway epithelial cells. J Virol **87:**3261–3270. http://dx.doi.org/10.1128/JVI.01956-12.
31. **Kallfass C, Lienenklaus S, Weiss S, Staeheli P.** 2013. Visualizing the beta interferon response in mice during infection with influenza A viruses expressing or lacking nonstructural protein 1. J Virol **87:**6925–6930. http://dx.doi.org/10.1128/JVI.00283-13.
32. **Jewell NA, Vaghefi N, Mertz SE, Akter P, Peebles RS, Jr, Bakaletz LO, Durbin RK, Flaño E, Durbin JE.** 2007. Differential type I interferon induction by respiratory syncytial virus and influenza A virus in vivo. J Virol **81:**9790–9800. http://dx.doi.org/10.1128/JVI.00530-07.
33. **Diebold SS, Kaisho T, Hemmi H, Akira S, Reis e Sousa C.** 2004. Innate antiviral responses by means of TLR7-mediated recognition of single-stranded RNA. Science **303:**1529–1531. http://dx.doi.org/10.1126/science.1093616.
34. **Culley FJ, Pennycook AM, Tregoning JS, Dodd JS, Walzl G, Wells TN, Hussell T, Openshaw PJ.** 2006. Role of CCL5 (RANTES) in viral lung disease. J Virol **80:**8151–8157. http://dx.doi.org/10.1128/JVI.00496-06.
35. **Jeyaseelan S, Manzer R, Young SK, Yamamoto M, Akira S, Mason RJ, Worthen GS.** 2005. Induction of CXCL5 during inflammation in the rodent lung involves activation of alveolar epithelium. Am J Respir Cell Mol Biol **32:**531–539. http://dx.doi.org/10.1165/rcmb.2005-0063OC.
36. **Kaminski MM, Ohnemus A, Cornitescu M, Staeheli P.** 2012. Plasmacytoid dendritic cells and Toll-like receptor 7-dependent signalling promote efficient protection of mice against highly virulent influenza A virus. J Gen Virol **93:**555–559. http://dx.doi.org/10.1099/vir.0.039065-0.
37. **Jeisy-Scott V, Davis WG, Patel JR, Bowzard JB, Shieh WJ, Zaki SR, Katz JM, Sambhara S.** 2011. Increased MDSC accumulation and Th2 biased response to influenza A virus infection in the absence of TLR7 in mice. PLoS One **6:**e25242. http://dx.doi.org/10.1371/journal.pone.0025242.
38. **Koyama S, Ishii KJ, Kumar H, Tanimoto T, Coban C, Uematsu S, Kawai T, Akira S.** 2007. Differential role of TLR- and RLR-signaling in the immune responses to influenza A virus infection and vaccination. J Immunol **179:**4711–4720. http://dx.doi.org/10.4049/jimmunol.179.7.4711.
39. **Pang IK, Pillai PS, Iwasaki A.** 2013. Efficient influenza A virus replication in the respiratory tract requires signals from TLR7 and RIG-I. Proc Natl Acad Sci U S A **110:**13910–13915. http://dx.doi.org/10.1073/pnas.1303275110.
40. **Liu Y, Mei J, Gonzales L, Yang G, Dai N, Wang P, Zhang P, Favara M, Malcolm KC, Guttentag S, Worthen GS.** 2011. IL-17A and TNF-alpha exert synergistic effects on expression of CXCL5 by alveolar type II cells in vivo and in vitro. J Immunol **186:**3197–3205. http://dx.doi.org/10.4049/jimmunol.1002016.
41. **Hui KP, Lee SM, Cheung CY, Mao H, Lai AK, Chan RW, Chan MC, Tu W, Guan Y, Lau YL, Peiris JS.** 2011. H5N1 influenza virus-induced mediators upregulate RIG-I in uninfected cells by paracrine effects contributing to amplified cytokine cascades. J Infect Dis **204:**1866–1878. http://dx.doi.org/10.1093/infdis/jir665.
42. **Guillot L, Le Goffic R, Bloch S, Escriou N, Akira S, Chignard M, Si-Tahar M.** 2005. Involvement of Toll-like receptor 3 in the immune response of lung epithelial cells to double-stranded RNA and influenza A virus. J Biol Chem **280:**5571–5580. http://dx.doi.org/10.1074/jbc.M410592200.
43. **Hemmi H, Kaisho T, Takeuchi O, Sato S, Sanjo H, Hoshino K, Horiuchi T, Tomizawa H, Takeda K, Akira S.** 2002. Small anti-viral compounds activate immune cells via the TLR7 MyD88-dependent signaling pathway. Nat Immunol **3:**196–200. http://dx.doi.org/10.1038/ni758.
44. **Sturn A, Quackenbush J, Trajanoski Z.** 2002. Genesis: cluster analysis of microarray data. Bioinformatics **18:**207–208. http://dx.doi.org/10.1093/bioinformatics/18.1.207.
45. **Cheadle C, Vawter MP, Freed WJ, Becker KG.** 2003. Analysis of microarray data using Z score transformation. J Mol Diagn **5:**73–81. http://dx.doi.org/10.1016/S1525-1578(10)60455-2.
46. **Nandakumar R, Finsterbusch K, Lipps C, Neumann B, Grashoff M, Nair S, Hochnadel I, Lienenklaus S, Wappler I, Steinmann E, Hauser H, Pietschmann T, Kröger A.** 2013. Hepatitis C virus replication in mouse cells is restricted by IFN-dependent and -independent mechanisms. Gastroenterology **145:**1414–1423. http://dx.doi.org/10.1053/j.gastro.2013.08.037.